

Effect of Organic Material on Field-scale Emissions of 1,3-Dichloropropene

S. R. Yates,* J. Knuteson, W. Zheng, and Q. Wang

Soil fumigation is important for growing many fruits and vegetable crops, but fumigant emissions may contaminate the atmosphere. A large-scale field experiment was initiated to test the hypothesis that adding composted municipal green waste to the soil surface in an agricultural field would reduce atmospheric emissions of the 1,3-dichloropropene (1,3-D) after shank injection at a 133 kg ha⁻¹ application rate. Three micrometeorological methods were used to obtain fumigant flux density and cumulative emission values. The volatilization rate was measured continuously for 16 d, and the daily peak volatilization rates for the three methods ranged from 12 to 24 µg m⁻² s⁻¹. The total 1,3-D mass that volatilized to the atmosphere was approximately 14 to 68 kg, or 3 to 8% of the applied active ingredient. This represents an approximately 75 to 90% reduction in the total emissions compared with other recent field, field-plot, and laboratory studies. Significant reductions in the volatilization of 1,3-D may be possible when composted municipal green waste is applied to an agricultural field. This methodology also provides a beneficial use and disposal mechanism for composted vegetative material.

AGRICULTURE HAS HELPED to sustain a growing population base worldwide with needed food and fiber (Borlaug, 2007). The availability of a stable and nutritious food supply significantly increases life expectancy and reduces illnesses related to malnutrition. Although agricultural activities provide a significant benefit to societies across the globe, many of these activities have the potential to produce adverse effects on environmental quality and human health. For example, regional air quality may be significantly affected from the use of pesticide chemicals (van den Berg et al., 1999). The potential impact is in the form of increases in toxic substances carried in the regional air stream as well as increases in ground-level ozone (i.e., photochemical smog) formed when reactive volatile organic chemicals (VOC) and nitrogen oxides (NO_x) are present in the atmosphere. This is a problem particularly during the summer months with high temperatures and sunny conditions.

In California, ozone formation has become a significant air-resource problem, and studies indicate that many locations throughout the state do not comply with USEPA's 8-h ozone standard (Neal et al., 2009). Because it is somewhat impractical to obtain spatially and temporally detailed measurements of ozone over such a large and diverse agricultural region, VOC emissions have become a proxy method to determine whether an area is in compliance with the ozone standard. Because agricultural operations may use methods that lead to the emission of VOCs to the atmosphere, restrictions are being developed to reduce VOC emissions to lower ground-level ozone to acceptable levels.

Data compiled by state regulatory agencies indicate that many mobile and stationary sources contribute to degrade regional air quality. In agricultural areas, the use of pesticides may be a significant component to the total VOC loading, and methods are needed to reduce emissions. Although pesticide VOC emissions are estimated to be a small fraction of the total over the entire state, in the central valleys, pesticide emissions have been estimated to contribute as much as 10% of the total. Reducing the agricultural contribution could yield significant benefit in these areas.

Copyright © 2011 by the American Society of Agronomy, Crop Science Society of America, and Soil Science Society of America. All rights reserved. No part of this periodical may be reproduced or transmitted in any form or by any means, electronic or mechanical, including photocopying, recording, or any information storage and retrieval system, without permission in writing from the publisher.

J. Environ. Qual. 40:1470–1479 (2011)

doi:10.2134/jeq2010.0206

Published online 7 Oct. 2010.

Received 3 May 2010.

*Corresponding author (scott.yates@ars.usda.gov).

© ASA, CSSA, SSSA

5585 Guilford Rd., Madison, WI 53711 USA

S.R. Yates, USDA–ARS, U.S. Salinity Lab., 450 W. Big Springs Rd., Riverside, CA 92507; J. Knuteson, formerly with Dow Agrosociences, now with FluxExperts, LLC, Indianapolis, IN; W. Zheng, now with Illinois Sustainable Technology Center, 1 E. Hazelwood Dr., Champaign, IL 61820; Q. Wang, current address: Delaware State Univ., Dover, DE 19901. The use of trade, firm, or corporation names in this research article is for the information and convenience of the reader. Such use does not constitute an official endorsement or approval by the United States Department of Agriculture or the Agricultural Research Service of any product or service to the exclusion of others that may be suitable. Assigned to Associate Editor Mingxin Guo.

Abbreviations: ADM, aerodynamic; 1,3-D, 1,3-dichloropropene; IHF, integrated horizontal flux; TPS, theoretical profile shape; VOC, volatile organic chemicals.

When there are insufficient data on emissions of volatile or semivolatile pesticides, current VOC inventories assume that the entire VOC portion of an applied material enters the atmosphere (Neal et al., 2009). This produces a worst-case estimate that overestimates atmospheric loading because all pesticides are subject to some level of irreversible sorption and degradation, which would reduce total emission. Although this may be a convenient approach, actual emission under field-relevant conditions could be significantly less, and regulations based on such an approach would needlessly affect growers. For some fumigants, information is available so that the VOC inventories can be adjusted to account for reduced emission resulting from application methodology and typical soil and atmospheric conditions.

Total emissions depend on a chemical's volatility, the soil's native ability to degrade chemicals, and the chemical residence time. Because soil fumigants have very high vapor pressures, rapid soil diffusion tends to result in significant volatilization. Soil fumigants also have relatively short degradation half-lives, so dissipation in soil can significantly reduce soil concentrations, which would reduce emissions (Yagi et al., 1995; Majewski et al., 1995; Yates et al., 1996).

To reduce the adverse impacts from fumigant use, many methods have been developed to reduce volatilization from soil. For example, the use of agricultural films (Wang et al., 1997; Gao and Trout, 2007; Papiernik et al., 2010), surface-applied fertilizers (Gan et al., 2000; Dungan et al., 2001), surface irrigation (McDonald et al., 2009; Ashworth and Yates, 2007), and organic amendments (Gan et al., 1998a; Dungan et al., 2005; McDonald et al., 2008) are among several methods being tested in an effort to use fumigant chemicals in an environmentally benign manner. For example, the use of repeated sprinkler irrigation has been shown to reduce gas-phase diffusion and has led to a reduction in emissions from 30 to 50% (Gan et al., 1998b; Gao et al., 2008; Yates et al., 2008) compared with standard practices. Amending the surface soil with organic material increases biotic and abiotic degradation, which leads to reduced emission. Although several laboratory and field plot experiments have been conducted that demonstrate the potential of this approach, no experimental information is available about the effectiveness at agronomic scales.

As regulators develop stricter rules to control regional ozone levels, activities with the potential to produce ozone will undoubtedly be adversely affected. Because information is lacking on pesticide emissions to the atmosphere, accurate measurements of the VOC (i.e., fumigant) losses from soil fumigation are needed, along with information on the effectiveness of new methods to reduce emissions.

A field experiment was conducted to test the hypothesis that emissions of 1,3-dichloropropene (1,3-D) after shank fumigation can be reduced by adding composted municipal green waste to the upper 15 cm of soil. There are few published reports of field experiments measuring emissions of 1,3-D after shank injection. To our knowledge, there are no reports of field experiments measuring field-scale emissions after adding composted municipal green waste to the surface soil. The experimental data reported from this study provide state regulators and the scientific community with important information on emissions from soils. An additional benefit of using organic

material from a municipal source is that it provides a disposal outlet for large quantities of low-value waste material and provides a beneficial use for growers at little or no cost.

Materials and Methods

The experimental site was located in an agricultural field near Buttonwillow, California. The soil consisted of a Milham sandy loam (fine-loamy, mixed, thermic Typic Haplargids), which typically has from 0.5 to 1% organic matter content in the upper 10 cm and decreasing value with depth. To improve soil fertility, the grower added 670 metric tons ha^{-1} (300 tons acre^{-1}) of composted municipal green waste to the field the previous year. The material was spread over the top of the field, and debris was removed. A moldboard plow was used to incorporate the green waste, and this was followed by several disking operations.

About 2 wk before the field experiment, the soil was plowed, followed by disking operations to break up soil aggregates. The field was irrigated and allowed to drain so that the initial water content of the soil was approximately 0.2 ($\text{cm}^3 \text{cm}^{-3}$). A commercial applicator applied Telone II (1,3-D, CAS: 542-75-6) (Dow Agrosiences, Indianapolis, IN) using an injection rig that carried a 450-cm tool bar with nine shanks. The shanks were spaced laterally in 50-cm increments and had a target depth of application of 46 cm (18 inches). The application rate was 133 kg ha^{-1} (12 gal acre^{-1}) and was applied to a nearly square area (178.4 m by 188.5 m) of 3.36 ha (8.3 acres). The total 1,3-D mass applied was 446.7 kg. The chemical was applied as 97.5% mixture of the *cis* (CAS: 10061-01-5) and *trans* (CAS: 10061-02-6) isomers; the remainder was comprised of inert components. The soil bulk density of the surface soil (0–10 cm) was $0.88 \pm 0.06 \text{ g cm}^{-3}$ and in the shank-injection zone (20–50 cm) was $1.41 \pm 0.13 \text{ g cm}^{-3}$. The experiment began on 31 Aug. 2005 and was concluded 16 d later. During this time, no irrigation water or precipitation was added to the field.

The reported soil degradation half-life for the Milham sandy loam is approximately 5 d (Ashworth and Yates, 2007). The organic carbon distribution coefficient for 1,3-D is $K_{oc} = 32 \text{ mL g}^{-1}$ (Wauchope et al., 1992), and the dimensionless Henry's Law constant is $K_h = 0.04$ to 0.06 (Leistra, 1970).

Air Measurements of 1,3-Dichloropropene

Atmospheric concentrations were obtained using charcoal sampling tubes (SKC 226-09; SKC, Inc., Fullerton, CA). A vacuum system was used to pull air through charcoal sampling tubes at $150 \text{ cm}^3 \text{ min}^{-1}$. The tubes contained two sections of charcoal: a front section with 400 mg and a second section with 200 mg. Before the experiment, several tests were conducted to show that 1,3-D would not break through the first bed of charcoal for the planned flow rates and sampling durations. The second section was tested for 1,3-D residues to verify that the chemical breakthrough did not occur under field conditions.

The sampling protocol involved removing the charcoal tubes from the sampling mast after each time interval, placing a cap on the ends of the tubes, storing the samples on ice, and transporting the sample to a nearby freezer for temporary storage. Several times during the experiment the samples were

transported to the laboratory in an ice chest and placed into a -80°C freezer and stored until analysis.

Samples of the 1,3-D concentrations in the soil gas phase were also collected at four locations in the field (Fig. 1). This was accomplished using stainless steel sampling tubes (outer diameter, 0.165 cm; inner diameter, 0.119 cm) installed to 15-, 30-, 45-, 60-, 75-, and 100-cm depths. A gas-tight syringe was connected to the stainless steel tube and used to create a vacuum to draw 50 mL of the soil pore air space and trap 1,3-D in a charcoal tube. Starting on Day 11, 500 mL of soil air space was sampled to increase the 1,3-D mass collected on the sorbent for analysis to ensure sufficient 1,3-D mass for residue analysis.

The 1,3-D concentration in the atmosphere was collected 12, 40, 80, 160, 236, and 359 cm above the soil surface. For the first 6 d of the experiment, the measurement periods were 2 h long during the daytime (0700–2100 h) and included a single nighttime sample. Starting on Days 7, 10, and 13, the daytime sampling intervals were increased to 3, 6, and 12 h, respectively. As the experiment progressed, the sampling periods were lengthened to ensure that sufficient mass was collected in the sampling tubes for residue analysis.

Meteorological Measurements

Wind speed measurements were obtained at five heights above the field (20, 40, 80, 160, 240 cm) using Thornthwaite anemometers (CWT-1806; C.W. Thornthwaite Assoc., Elmer, NJ). In addition, wind speed measurements were collected at 297 cm using a MetOne Wind Set (034B; Campbell Scientific Inc., Logan, UT). Pairs of fine-wire thermocouples (FW3; Campbell Scientific, Inc.), placed at 40- and 80-cm heights, were used to measure the air temperature gradient. Relative humidity and temperature (HMP35C; Campbell Scientific, Inc.), incoming solar radiation (LI-200S; LI-COR, Inc., Lincoln, NE), net solar radiation (Q-6; Radiation and Energy Balance Systems, Inc., Seattle, WA), and barometric pressure (Vaisala PTA-427; Campbell Scientific, Inc.) measurements were also obtained throughout the experiment. A schematic of the field layout is shown in (Fig. 1).

Solar and net radiations were collected as hourly averages of instrument measurements taken every 5 s. This yielded a nominal time series of 360 values (i.e., $24\text{ h} \times 15$ daily values). Using the 15 daily values occurring at a particular hour, an average and standard deviation were calculated to represent a

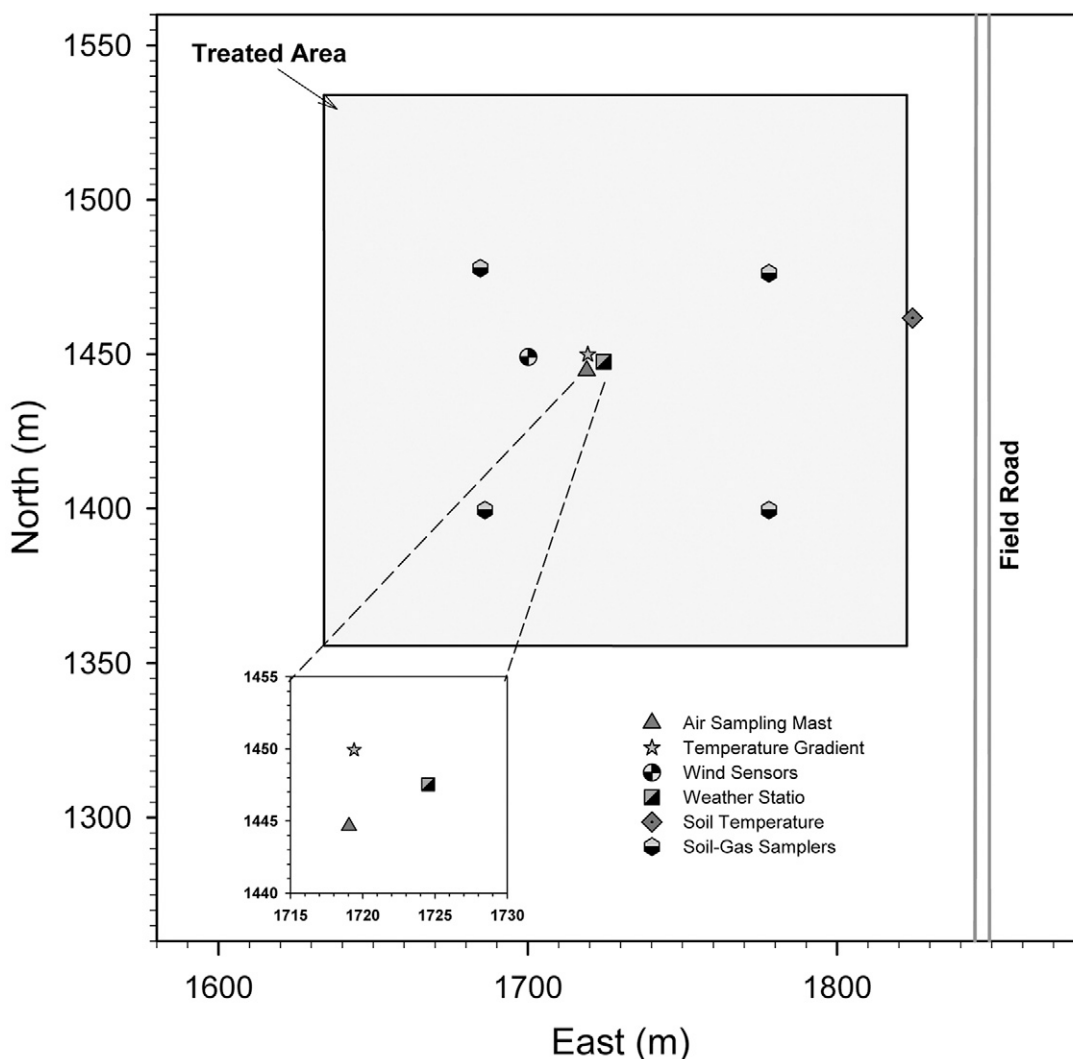


Fig. 1. Schematic of the field site showing the position of sensors and field dimensions.

typical hour of the day. This resulted in 24 average solar and net radiations and their standard deviations.

Methods for Measuring the Volatilization Rate

Three micrometeorological methods were used to compute the volatilization rate: aerodynamic (Parmele et al., 1972), integrated horizontal flux (Denmead et al., 1977), and theoretical profiles shape (Wilson et al., 1982) methods. A volatilization rate, $f_z(0, t)$, based on the aerodynamic method, requires gradients of wind speed, temperature, and 1,3-D concentration (Parmele et al., 1972) collected over a relatively large and spatially uniform source area. It is customary to place the instruments at a height that is approximately 1 to 2% of the upwind fetch distance (Rosenberg et al., 1983), which for this case would be between the 0- and 90-cm heights. The equation used for the aerodynamic calculation is:

$$f_z(0, t) = k^2 \frac{(\bar{C}_1(t) - \bar{C}_2(t))(\bar{u}_2(t) - \bar{u}_1(t))}{\phi_m(t)\phi_c(t) \ln(z_2/z_1)^2} \quad [1]$$

where $u_1(t)$ and $C_1(t)$ are the wind speed and concentration at height z_1 , respectively; k is von Karman's constant; and ϕ are stability corrections. The equations used for ϕ are (Pruitt et al., 1973)

$$\begin{aligned} \phi_m &= (1 - 16Ri)^{-0.33} & \phi_c &= 0.885(1 - 22Ri)^{-0.4} \\ Ri &< 0 \\ \phi_m &= (1 + 16Ri)^{0.33} & \phi_c &= 0.885(1 + 34Ri)^{0.4} \\ Ri &> 0 \end{aligned} \quad [2]$$

where the subscripts m and c indicate momentum and chemical, respectively; Ri is the gradient Richardson number (see Eq. [3]); g is the acceleration due to gravity; and T is the absolute temperature (K).

$$Ri = \frac{g}{T} \left(\frac{\partial T}{\partial z} \right) \left(\frac{\partial u}{\partial z} \right)^{-2} \quad [3]$$

The integrated horizontal flux (IHF) method (Denmead et al., 1977) uses concentrations and horizontal wind speed measurements at several heights above the soil surface. The methodology assumes that the 1,3-D mass emitted from a spatially uniform surface area upwind from a sampling mast is equal to the mass that is collected along a vertical plane at the sampling point. This method uses principals of mass balance to estimate the volatilization rate and has the advantage that corrections for atmospheric stability are not needed. The volatilization rate is determined using Eq. [4]:

$$f_z(0, t) = \frac{1}{L} \int_{\xi_{u=0}}^{\infty} \bar{u}(\xi) \bar{C}(\xi) d\xi \quad [4]$$

where L is the length from the sampling location to the upwind edge of the treated area.

The third approach—the theoretical profile shape method—uses the trajectory simulation model Wilson et al. (1982) to estimate the volatilization rate:

$$f_z(0, t) = \left. \frac{\bar{u}(t) \bar{C}(t)}{R_{inst}} \right|_{z_{inst}} \quad [5]$$

where Z_{inst} is the instrument height ($Z_{inst} = 2.15$ m), and R_{inst} is the ratio of the horizontal to vertical flux determined from the trajectory simulation model ($R_{inst} = 13.75$) (Wilson et al., 1981). This requires measurements of the concentration and wind speed at a single height above the soil surface, and the height depends on the surface roughness and friction velocity. An advantage of this method is that it does not require large fetch distances and is relatively insensitive to atmospheric stability, so temperature and wind gradients and stability corrections are unnecessary. Further information on these approaches can be found elsewhere (e.g., Parmele et al., 1972; Wilson et al., 1982; Majewski et al., 1995; Yates et al., 1996; Yates et al., 2008).

The total mass volatilized from soil as a function of time since application can be found using Eq. [6]:

$$f_{total}(t) = \iint_{x,y} \int_0^t f_z(x, y, 0, \tau) d\tau dy dx = A \int_0^t f_z(0, \tau) d\tau \quad [6]$$

where $f_z(x, y, 0, \tau)$ is the volatilization flux density ($\mu\text{g m}^{-2} \text{s}^{-1}$), τ represents the time coordinate, and (x, y) is a horizontal coordinate in the treated region of the field. For a spatially uniform source, the right-hand equation can be used, where A is the area (m^2) of the treated field.

Chemical Analysis

A sampling tube from the freezer was warmed to room temperature and cut, and each charcoal bed was transferred to an individual 10-mL head-space vial. Then, 3 mL of acetone was added, and each vial was immediately sealed with an aluminum cap with a Teflon-lined septum. The vials were shaken for 30 min in a reciprocating shaker, after which 1 mL of the acetone supernatant was transferred to a 2-mL GC-vial, capped, and stored at -70°C until analysis.

A gas chromatograph (Agilent 6890; Agilent Technologies, Palo Alto, CA) with a micro-electron capture detector and DB-VRX column (30 m by 0.25 mm) was used for the 1,3-D analysis. The inlet and detector temperatures were set at 240 and 290°C , respectively. The temperature program held an initial temperature of 50°C for 1 min, was increased to 80°C at $4.0^\circ\text{C min}^{-1}$ where it remained for 2 min, and was increased from 80 to 120°C at $30^\circ\text{C min}^{-1}$ and remained for 2 min. The injection volume and the split ratio were 2.0 μL and 20:1, respectively. Nitrogen at a flow rate of 60 mL min^{-1} was used for the makeup gas.

The limit of quantification and the limit of detection were 0.05 μg per tube and 0.015 μg per tube, respectively. The extraction efficiency of the charcoal sampling tubes for an airflow rate of 150 $\text{cm}^3 \text{min}^{-1}$ was determined from repeated tests conducted at 1, 5, 10, and 1810 times the limit of quantification. The extraction efficiency was found to be $84 \pm 7\%$ (1,3-D *cis*) and $86 \pm 7\%$ (1,3-D *trans*). Due to the high extraction efficiency, the fumigant concentration values are reported without adjustment. After connecting

four sampling tubes in series and sampling for 8 h, it was found that more than 99.99% of the total mass was contained in the first tube. Three sets of travel samples at three concentration levels were prepared to ensure no significant chemical loss occurred during sample handling, transportation, and storage. The difference between travel samples and the standards was less than $0.005 \pm 0.009\%$.

Results and Discussion

Environmental Conditions

The typical summer weather in the Buttonwillow region includes high temperatures and cloudless conditions and nearly constant daytime wind directions. At times, windblown dust may reduce incident solar radiation, but this did not occur during the experiment. Figure 2 contains hourly means and standard deviations of the solar irradiance and net solar radiation during the experiment. For a particular hour of the day, the measurement values were found to be nearly the same throughout the experiment. Noting the small standard deviation for solar irradiance, it is clear that the incident radiation was relatively uniform and cyclic during the experiment, which is indicative of continuously clear-sky conditions. The maximum and average of the solar radiation measurements were 881 and 264 W m^{-2} , respectively. Like the solar irradiance, the net radiation was found to be a smoothly varying throughout the day, and the daily patterns were highly uniform during this experiment. The maximum, minimum, and average values were 478, -79 , and 97 W m^{-2} , respectively.

Figure 3A shows the ambient air temperature 40 cm above the soil surface. During the first 16 d of the experiment, the maximum temperature was approximately 37.3°C , daily minimum temperature was 11.6°C , and the average temperature

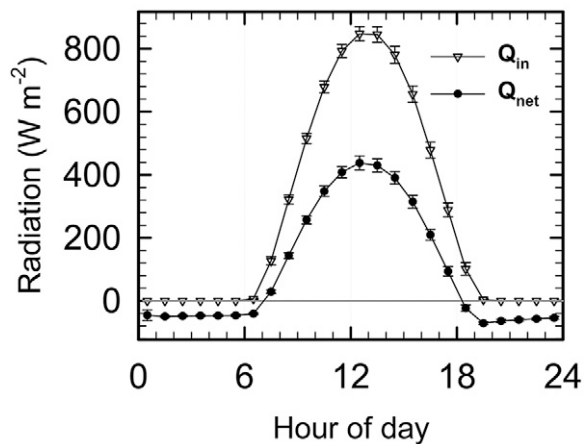


Fig. 2. Global solar irradiance (W m^{-2}) and net radiation (W m^{-2}) as a function of time of day. The point values are averages of the hourly radiation over the entire experiment. Error bars are the standard deviations. Small standard deviations are indicative of relatively uniform clear sky conditions.

was 24.0°C . Starting on Day 9, a slight cooling trend began, with temperatures increasing gradually for the next several days (maximum, minimum, and mean were 30.7 , 8.3 , and 18.7°C , respectively).

Figure 3 shows the wind speed at 40 cm above the surface (Fig. 3B) during the experiment and a wind-rose diagram (Fig. 3C), which provides information about the frequency that the winds occur in a particular direction. The winds moved predominantly from the north to the south (Fig. 3C); the dashed circles in Fig. 3C indicate that 17.4% of the time the wind direction is ± 11.25 degrees from due north and that the wind speeds are usually from 1.5 to 3.0 m s^{-1} . This wind-rose diagram was created using 2-min wind speed and wind direction data and indicates that occasionally winds in excess

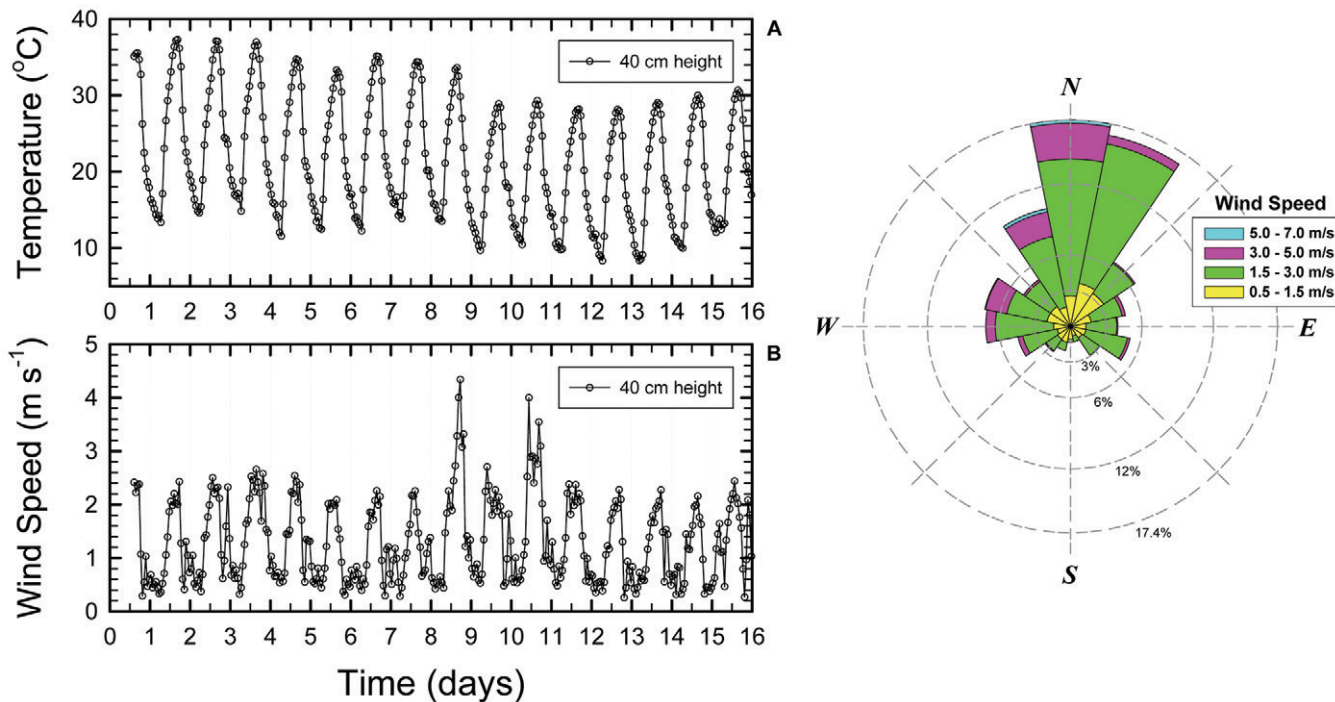


Fig. 3. (A) Air temperature ($^\circ\text{C}$) and (B) wind speed (m s^{-1}) at 40 cm above the soil surface during the experiment. Integer values occur at midnight. (C) A wind rose diagram shows the wind direction, wind speed, and probability the wind will occur in a specific direction.

of 5 m s^{-1} were observed. On an hourly averaged basis, the maximum wind speed was 4.3 m s^{-1} , but daily maxima were generally between 2 and 3 m s^{-1} . During the middle of the night, wind speeds were commonly from 0.2 to 0.6 m s^{-1} .

Figure 4 is a graph of the temperature gradient, Richardson's number, and atmospheric stability parameter for momentum. The temperature gradient was obtained from measurements collected at 80 and 40 cm above the soil surface, and negative values indicate higher temperatures near the soil surface. During the sampling period, the observed temperature gradient varied by approximately $\pm 1^\circ\text{C}$, with an occasional value approaching $+2^\circ\text{C}$. Also, negative gradients occurred during the day, which is indicative of unstable atmospheric conditions. During the daylight hours, the temperature gradient increases from approximately zero an hour after sunrise to a maximum negative value at solar noon and then decreases to zero an hour before sunset. During the nighttime, the temperature gradient has positive values, but the gradient is much more erratic compared with daytime values.

The gradient Richardson number, Ri , provides a means to determine the effect of thermal stability on the shape of the wind speed profile and on turbulent exchange (Fig. 4B). The Ri provides information on the relative importance of buoyancy and mechanical forces on fumigant movement in the atmosphere. A value of Ri near zero indicates near-neutral conditions, negative values indicate unstable conditions, and positive values occur for stable atmospheric conditions.

Figure 4C shows the stability parameter for momentum, ϕ_m . Because ϕ_m is in the denominator of Eq. [1], this parameter tends to increase the emission rate when it has values < 1 . In general, $0 < \phi_m < 1$ when Richardson's number is less than zero. For these time periods, unstable conditions generally lead to increased volatilization because the air over the soil surface is warmer than the air above and therefore rises. This causes the fumigant to move away from the soil surface and tends to increase the concentration gradient across the soil-atmosphere boundary. This can be a factor driving the volatilization process. At night, when the stability parameter is > 1 , the stable atmosphere tends to produce higher concentrations near the soil surface, which reduces gradients and the volatilization rate.

Air Concentrations

The effect of atmospheric stability, Φ_m , and turbulence on 1,3-D concentration in the atmosphere can be seen in Fig. 5 at 40 and 80 cm above the soil surface. Nighttime concentrations tend to be much higher than midday values. Also, the concentration levels were relatively high during the first 4 d of the experiment and were much lower after about 6 d. At 40 cm above the soil surface, observed concentrations exceeded $400 \mu\text{g m}^{-3}$ and had a peak value of nearly $500 \mu\text{g m}^{-3}$. At a height

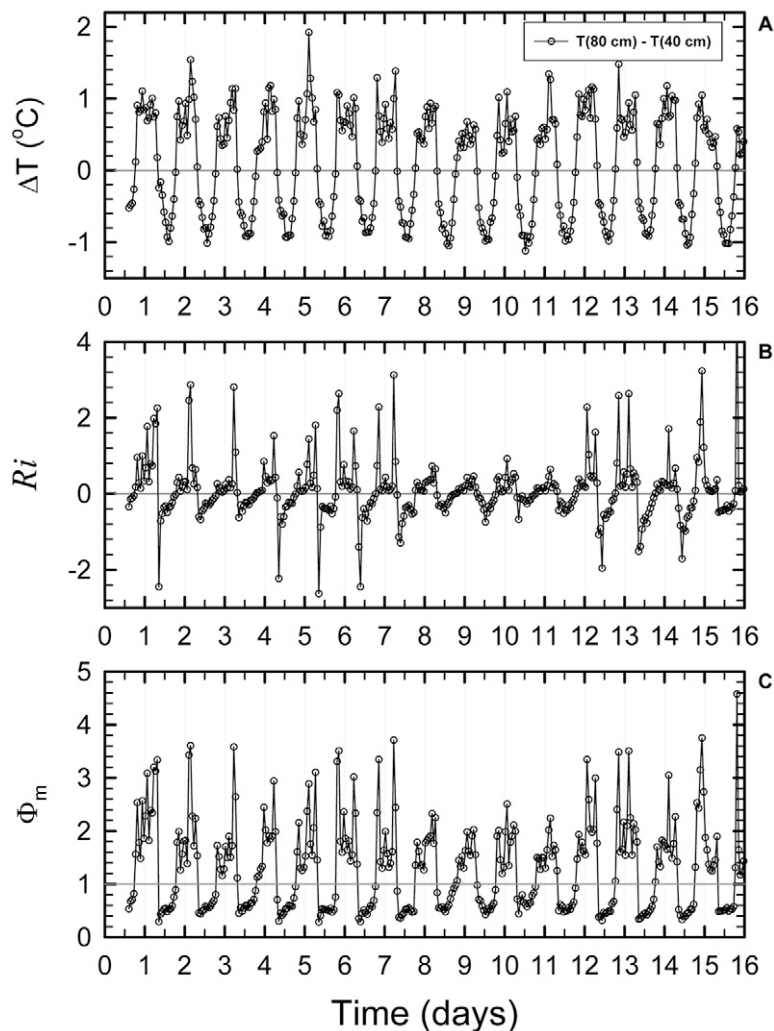


Fig. 4. (A) Temperature difference (ΔT), (B) gradient Richardson's number (Ri), and (C) atmospheric stability parameter (ϕ_m) for momentum during the experiment.

of 80 cm above the soil surface, the concentration remained below $130 \mu\text{g m}^{-3}$.

The large concentrations at the beginning of the experiment are due to a combination of factors, including a larger source of chemical present in the soil, a larger concentration gradient directed toward the soil surface, and rapid upward diffusion caused by the presence of soil fracture zones caused by the fumigation shanks. The shanks have been shown to create a more uniform soil concentration and higher concentrations near the soil surface compared with injection methods that do not produce a soil fracture (Yates, 2009). As time advances, the fumigant volatilizes and degrades in soil, so atmospheric concentrations lessen.

1,3-Dichloropropene Volatilization

Figure 6 shows time series for the three methods used to calculate the volatilization rate (flux density), which includes the aerodynamic (ADM), IHF, and the theoretical profile shape (TPS) methods. These three methods demonstrate a similar overall pattern of high rates early in the experiment and low rates at about 5 to 6 d after application. At a particular time point, the three methods produce a range of volatilization

rates, and occasionally the ADM method is three to five times higher than the IHF and TPS methods.

The aerodynamic method produced a maximum period-averaged volatilization rate of $23 \mu\text{g m}^{-2} \text{s}^{-1}$, which occurred at 3.58 d (2.9 d after application). Before this, two other large volatilization rates were computed at 1.3 d ($12 \mu\text{g m}^{-2} \text{s}^{-1}$) and 2.3 d ($13 \mu\text{g m}^{-2} \text{s}^{-1}$). For the IHF method, the peak volatilization rate also occurred at 3.58 d ($4.1 \mu\text{g m}^{-2} \text{s}^{-1}$), and for the TPS method, the peak flux occurred at 1.75 d ($4.4 \mu\text{g m}^{-2} \text{s}^{-1}$). Generally, the three methods provide similar volatilization rates except at four time points, where the ADM method estimates higher rates compared with the IHF and TPS methods.

The flux rates obtained with the ADM tend to be fairly sensitive to the atmospheric stability parameters ϕ_m and ϕ_c (see Eq. [1]). The values of ϕ_m and ϕ_c were <1 during the middle of each day of the experiment and were >1 each night; these values would generally lead to higher flux rates during the daytime and be lower values at night. However, this generalized behavior was not observed during the first 3 d of the experiment (Fig. 6), indicating that other processes were effecting the emission rate.

Also shown in Fig. 6 (inset) is the total 1,3-D emission from soil as a function of time after application. It is clear from the proximity of the curves that the IHF and TPS methods provide estimated volatilization rates that are very similar; with estimated cumulative values of 3.3 and 3.4%, respectively. The estimate of the cumulative emission from the ADM (8.2%) is larger compared with the other methods. The difference between methodologies represents approximately 5% based on the amount of 1,3-D applied to the field. This is similar to the results of Yates et al. (2008) for a different field experiment conducted at the same time and in the vicinity of this study described herein.

The deviation between methodologies shown in Fig. 6 is consistent with studies of the experimental uncertainty for flux estimation methods (Majewski, 1997; Wilson and Shum, 1992). These studies showed that the experimental and theoretical accuracy of the flux estimates should be in the range of ± 20 to 50%. One approach for estimating uncertainty was based on a regression analysis of the log-linear wind speeds and concentrations with respect to height (Majewski, 1997). This analysis found that the uncertainty for methyl bromide emissions was approximately $\pm 50\%$. It would be reasonable to expect that this analysis should apply to other fumigants that have log-linear concentration profiles. Wilson and Shum (1992) conducted an uncertainty analysis for the IHF method and found that the theoretical accuracy was approximately $\pm 20\%$, provided

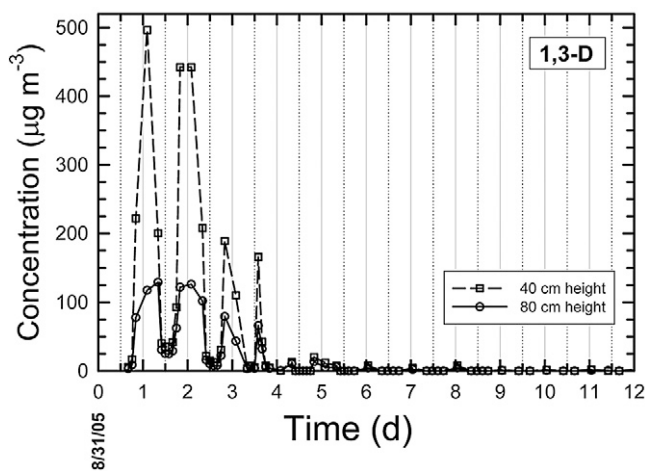


Fig. 5. Measured 1,3-dichloropropene (1,3-D) concentration in the atmosphere at 40 and 80 cm above the soil surface during the first 12 d of the experiment.

that the field site was sufficiently large. The estimate of the uncertainty was obtained using a Lagrangian stochastic model and also provides guidelines that can be used in the design of field experiments.

Under typical shank injection, the observed daily peak volatilization rates often occur during midday (Majewski et al., 1995; Yates et al., 1996; van Wesenbeeck et al., 2007). Although high daytime flux rates are common, some experiments have found the daily peak flux to occur at other times during a day (Yates et al., 1997; Sullivan et al., 2004). For this experiment, higher flux values were observed during the night and morning. This is a period usually characterized by stable atmospheric conditions and occurs before the soil

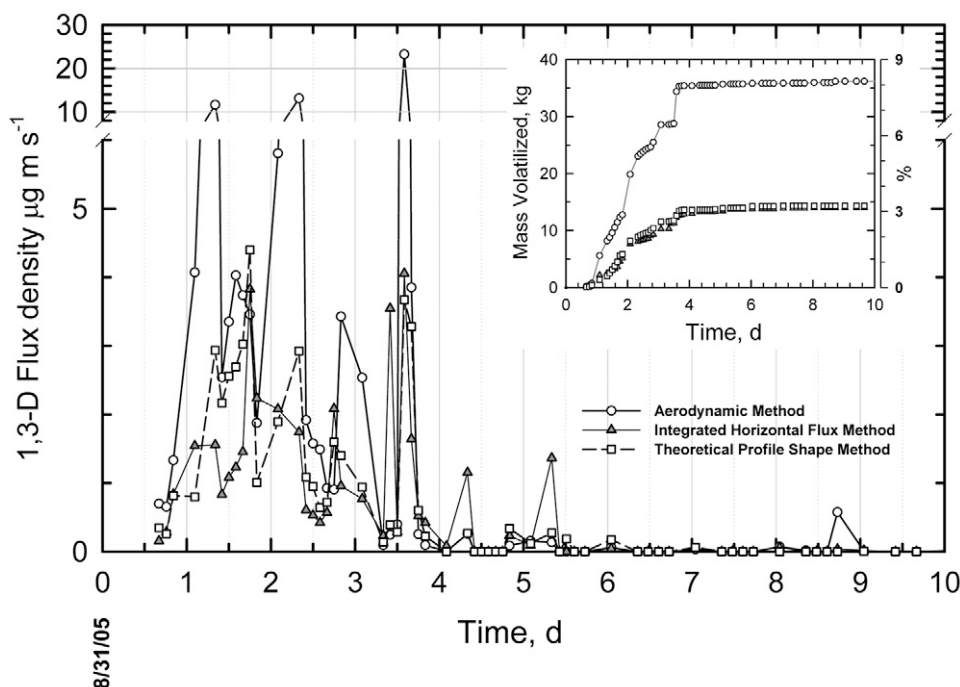


Fig. 6. Volatilization rate ($\mu\text{g m}^{-2} \text{s}^{-1}$) as a function of time (day) after application for the aerodynamic (solid line, circles), integrated horizontal flux (solid line, triangles), and theoretical profile shape (dashed line, squares) during the first 10 d of the experiment. Values after 10 d were essentially zero. The inset shows cumulative 1,3-dichloropropene (1,3-D) emission as a function of time after application. The percentages on the right-most axis of the inset shows the percent of applied 1,3-D.

surface is heated by solar radiation. With the exception of Day 3, lower flux values were observed at midday and early afternoon during this study. Low midday flux rates were also observed at another field experiment conducted nearby (Yates et al., 2008). However, in this latter experiment, the low flux rates were attributed to sprinkler irrigation sealing the soil surface just before noon during the first 5 d after fumigant application.

Similar observations of low midday flux rates have been attributed to soil heating and a reduction in soil water content leading to increases in vapor adsorption (Glotfelty et al., 1984, 1989; Pennell et al., 1992; Chen et al., 2000; Bedos et al., 2009). For a situation where a soil surface becomes very dry during the day and wetter during the night and morning hours due to water movement and condensation at the surface, the daytime drying increases vapor phase adsorption to the soil particles and organic material present in the upper soil layer. Vapor phase adsorption has been shown to strongly bind volatile pesticides to soil particles in a highly nonlinear process as water contents decreases (Goss, 1992; Goss and Eisenreich, 1996). Research has also shown that the water content of the surface soil layer fluctuates due to heating and cooling of the soil. This can be interpreted to be a result of evaporation and the movement of water vapor due to changes in the thermal regime in soil (Jackson et al., 1973; Zheng et al., 2009). Visually, the soil was very dry and powdery during midday, so vapor adsorption could have been highest during this time.

Accurate information of fumigant emissions is of importance to state and federal regulators because atmospheric loadings are used to determine various environmental risk endpoints. For issues related to bystander exposure and public health, the short-term emission rate is needed to determine the risk associated with transient high-level emission events. These events may lead to unacceptable exposure to pesticide vapors. To determine the effect of VOC emissions on near-surface ozone, the total atmospheric loading is a useful indicator of soil fumigation's contribution to regional VOC, which may participate in ozone formation.

For the purposes of verification, soil was collected from the field site for use in a laboratory study (Ashworth and Yates, 2007). The experiment was conducted using 1.5-m stainless steel soil columns that were placed in a controlled temperature environment so that the observed temperature conditions at the field site could be closely simulated. This study reported that the total emissions of *cis*-1,3-D after 14 d were 33.1% for soil collected in a nearby field that did not receive municipal green waste and 5.7% for soil collected from the field described herein. This estimate is smaller compared with the estimated total *cis*-1,3-D emission (Table 1)

using the aerodynamic method (9.7%) and is larger than the total *cis*-1,3-D emissions estimates from the TPS and IHF methods (3.8–3.9%). The average of the three field-scale flux estimates compares very well with the laboratory value of 5.8%. When compared with the total emission estimate from the laboratory treatment that did not contain organic material (33.1%), the total emission estimates for the field-scale and laboratory experiments demonstrate that significant reduction in emission is possible using composted municipal green waste as a soil amendment.

Several other field-plot and laboratory studies have found that the addition of organic material to surface soil reduces emissions of 1,3-D. Dungan et al. (2005) conducted a field plot experiment on raised beds (5 m by 1 m by 0.15 m) and found that steer manure or chicken manure, respectively, incorporated into the top 5 cm of the bed would result in emissions of 1,3-D that were 48 and 28% less than the unamended control plot. They also found that the measured reduction in emissions did not change after increasing the rate at which organic material was applied from 5 to 10%. Gan et al. (1998a) found that total emissions of 1,3-D were reduced from 30 to 16% by the addition of 5% organic matter to the top 5 cm of a soil column. In a laboratory column study, McDonald et al. (2008) found that the addition of 5% organic material (steer manure) to the upper 5 cm of the soil reduced emissions from 51 to 29%. Gao et al. (2009) found that the addition of dairy manure alone did not significantly reduce total emissions of 1,3-D. However, the measured total emission rate for this study was much higher than commonly observed (~80% loss) in field and field-plot studies.

Many reports investigating the effect of adding organic material to the surface before soil fumigation demonstrate that emissions can be reduced by 40% or more. The type of organic material is a factor in how effective this methodology will be in reducing emissions.

Soil Gas Phase 1,3-Dichloropropene Concentration

Figure 7 is a graph of the soil gas-phase concentration at various times after application of 1,3-D. At the first sampling, the concentration of the soil gas phase at 45 cm depth was approximately 29 $\mu\text{g cm}^{-3}$, and the soil zone that had significant 1,3-D concentration was between 30 and 60 cm. On consecutive days, the peak concentration decreased and the treatment zone increased to approximately 80 cm.

Yates et al. (2008) observed similar soil gas concentrations in their experiment conducted at the same time in an adjacent field that did not receive composted green waste. For example, concentrations at 45 cm depth on Days 1, 2, 3, 4, and 11 were 25.5, 13.0, 6.6, 3.93, and 0.038 $\mu\text{g cm}^{-3}$, respectively (Yates et al., 2008). In Fig. 7, the soil gas

Table 1. Total emissions and percent of applied of 1,3-dichloropropene (total mass applied was 447 kg).

Method	<i>cis</i> -1,3-D†		<i>trans</i> -1,3-D		1,3-D	
	Total emissions	% Applied	Total emissions	% Applied	Total emissions	% Applied
	kg		kg		kg	
Aerodynamic	21.7	9.7	14.8	6.6	36.5	8.2
Integrated horizontal flux	8.7	3.9	6.4	2.9	15.1	3.4
Theoretical profile shape	8.5	3.8	6.2	2.8	14.6	3.3

† 1,3-D, 1,3-dichloropropene.

concentrations at 45 cm for Days 1, 2, 3, and 4 were 29.0, 11.7, 4.57, and 2.05 $\mu\text{g cm}^{-3}$, respectively. It appears that surface application of organic material did not markedly affect soil gas concentration at depth when compared with a fumigation that included sequential sprinkler irrigations. The effect of composted green waste on fumigant efficacy remains uncertain, and additional research is warranted. Fumigant emissions were significantly reduced, so this approach could be beneficial in reducing atmospheric loading of fumigant VOCs, providing material to crop land that improves soil tilth and nutrient levels and providing an outlet for municipalities to dispose of large quantities of green waste material that are often otherwise destined for disposal in land fills.

This study demonstrates the benefit of amending soil with composted municipal green waste as a means to reduce emissions of 1,3-D after preplant soil fumigation. Application of green waste at a rate of 670 metric tons ha^{-1} (300 tons acre^{-1}) reduced total 1,3-D from 33% (Ashworth and Yates, 2007) to approximately 5% of the applied fumigant. Based on recent laboratory and field experiments conducted under similar soil and environmental conditions, it appears that atmospheric emissions of 1,3-D can be reduced by 40 to 80% compared with conventional application methods. Further research is needed to determine how soil and atmospheric conditions contribute to reducing emissions. If further testing confirms these results, this approach can provide a simple, environmentally beneficial, effective, and relatively low-cost method to protect the environment from agricultural chemicals and to reduce VOC emissions to the atmosphere.

Acknowledgments

The authors thank Q. Zhang, Fred Ernst, J. Jobes and A. Khan for their assistance with the experiment. Part of the research described was supported by the California Air Resources Board (agreement #05-351).

References

- Ashworth, D.J., and S.R. Yates. 2007. Surface irrigation reduces the emission of volatile 1,3-D from agricultural soils. *Environ. Sci. Technol.* 41:2231–2236.
- Bedos, C., S. Ge'nermont, E. Le Cadre, L. Garcia, E. Barriuso, and P. Cellier. 2009. Modelling pesticide volatilization after soil application using the mechanistic model Volt'Air. *Atmos. Environ.* 43:3630–3639.
- Borlaug, N. 2007. Feeding a hungry world. *Science* 318:359.
- Chen, D., D.E. Rolston, and T. Yamaguchi. 2000. Calculating partition coefficients of organic vapors in unsaturated soil and clays. *Soil Sci.* 165:217–225.
- Denmead, O.T., J.R. Simpson, and J.R. Freney. 1977. A direct field measurement of ammonia emission after injection of anhydrous ammonia. *Soil Sci. Soc. Am. J.* 41:1001–1004.
- Dungan, R., J. Gan, and S.R. Yates. 2001. Effect of temperature, organic amendment rate, and moisture content on the degradation of 1,3-dichloropropene in soil. *Pest Manag. Sci.* 57:1–7.
- Dungan, R.S., S.K. Papiernik, and S.R. Yates. 2005. Use of composted animal manures to reduce 1,3-dichloropropene emissions. *J. Environ. Sci. Health B* 40:355–362.
- Gan, J., J.O. Becker, F.F. Ernst, C. Hutchinson, and S.R. Yates. 2000. Surface application of ammonium thiosulfate fertilizer to reduce volatilization of 1,3-dichloropropene from soil. *Pest Manag. Sci.* 56:264–270.
- Gan, J., S.R. Yates, D. Crowley, and J.O. Becker. 1998a. Acceleration of 1,3-dichloropropene degradation by organic amendments and potential application for emissions reduction. *J. Environ. Qual.* 27:408–414.

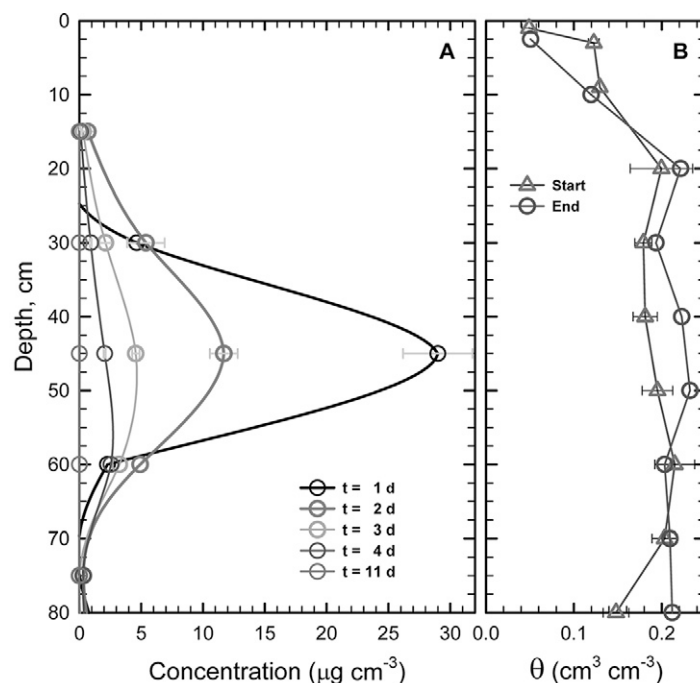


Fig. 7. (A) Soil gas phase concentration ($\mu\text{g cm}^{-3}$) with depth in soil. Each line represents the concentration distribution at a particular time after application. Error bars are provided on the curves to give an indication of the variability at the four sampling locations. (B) Soil water content ($\text{cm}^3 \text{cm}^{-3}$) with depth before fumigation and at the end of the experiment.

- Gan, J., S.R. Yates, D. Wang, and F.F. Ernst. 1998b. Effect of application methods on 1,3-dichloropropene volatilization from soil under controlled conditions. *J. Environ. Qual.* 27:432–438.
- Gao, S., R. Qin, B.D. Hanson, N. Tharayil, T.J. Trout, D. Wang, and J. Gerik. 2009. Effects of manure and water applications on 1,3-dichloropropene and chloropicrin emissions in a field trial. *J. Agric. Food Chem.* 57:5428–5434.
- Gao, S., and T.J. Trout. 2007. Surface seals reduce 1,3-dichloropropene and chloropicrin emissions in field tests. *J. Environ. Qual.* 36:110–119.
- Gao, S., T.J. Trout, and S. Schneider. 2008. Evaluation of fumigation and surface seal methods on fumigant emissions in an orchard replant field. *J. Environ. Qual.* 37:369–377.
- Glotfelty, D.E., A.W. Taylor, B.C. Turner, and W.H. Zoller. 1984. Volatilization of surface-applied pesticides from fallow soil. *J. Agric. Food Chem.* 32:638–643.
- Glotfelty, D.E., M.M. Leech, J. Jersey, and A.W. Taylor. 1989. Volatilization and wind erosion of soil surface applied atrazine, simazine, alachlor, and toxaphene. *J. Agric. Food Chem.* 32:546–551.
- Goss, K.-U. 1992. Effects of temperature and relative humidity on the sorption of organic vapors on quartz sand. *Environ. Sci. Technol.* 26:2287–2294.
- Goss, K.-U., and S.J. Eisenreich. 1996. Adsorption of VOCs from the gas phase to different minerals and a mineral mixture. *Environ. Sci. Technol.* 30:2135–2142.
- Jackson, R.D., B.A. Kimball, R.J. Reginato, and F.S. Nakayama. 1973. Diurnal soil-water evaporation: Time-depth-flux patterns. *Soil Sci. Soc. Am. J.* 37:505–509.
- Leistra, M. Distribution of 1,3-dichloropropene over the phases in soil. 1970. *J. Agric. Food Chem.* 18:1124–1126.
- Majewski, M.S. 1997. Error evaluation of methyl bromide aerodynamic flux measurements. p. 135–153. *In* J.N. Seiber, J.A. Knuteson, J.E. Woodrow, N.L. Wolfe, M.V. Yates, and S.R. Yates (ed.) *Fumigants: Environmental fate, exposure, and analysis*. ACS Symposium Series 652, American Chemical Society, Washington, DC.
- Majewski, M.S., M.M. McChesney, J.E. Woodrow, J.H. Prueger, and J.N. Seiber. 1995. Aerodynamic measurements of methyl bromide volatilization from tarped and nontarped fields. *J. Environ. Qual.* 24:742–751.
- McDonald, J.A., S. Gao, R. Qin, B. Hanson, T. Trout, and D. Wang. 2009. Effect of water seal on reducing 1,3-dichloropropene emissions from different soil textures. *J. Environ. Qual.* 38:712–718.
- McDonald, J.A., S. Gao, R. Qin, and J. Thomas. 2008. Thiosulfate and manure amendment with water application and tarp on 1,3-dichloropropene

- lene emission reductions. *Environ. Sci. Technol.* 42:398–402.
- Neal, R., F. Spurlock, and R. Segawa. 2009. Annual report on volatile organic chemical emissions from pesticides: Emissions for 1990–2007. Report EH09-01 (March 2009), California Environmental Protection Agency, Sacramento, CA.
- Papiernik, S.K., S.R. Yates, and D.O. Chellemi. 2010. A standardized approach for estimating the permeability of plastic films to soil fumigants under various field and environmental conditions. *J. Environ. Qual.* doi:10.2134/jeq2010.0118.
- Parmele, L.H., E.R. Lemon, and A.W. Taylor. 1972. Micrometeorological measurement of pesticide vapor flux from bare soil and corn under field conditions. *Water Air Soil Pollut.* 1:433–451.
- Pennell, K.D., R.D. Rhue, P.S.C. Rao, and C.T. Johnston. 1992. Vapor-phase sorption of p-xylene and water on soils and clay minerals. *Environ. Sci. Technol.* 26:756–763.
- Pruitt, W.O., D.L. Morgan, and F.J. Lourence. 1973. Momentum and mass transfers in the surface boundary layer. *Q. J. R. Meteorol. Soc.* 99:370–386.
- Rosenberg, N.J., B.L. Blad, and S.B. Verma. 1983. *Microclimate: The biological environment.* John Wiley & Sons, New York.
- Sullivan, D.A., M.T. Holdsworth, and D.J. Hlinka. 2004. Control of off-gassing rates of methyl isothiocyanate from the application of metam-sodium by chemigation and shank injection. *Atmos. Environ.* 38:2457–2470.
- van den Berg, F., R. Kubiak, W. Benjey, M. Majewski, S.R. Yates, G. Reeves, J. Smelt, and A. van der Linden. 1999. Emission of pesticides into the air. *Water Air Soil Pollut.* 115:195–218.
- van Wesenbeeck, I.J., J.A. Knuteson, D.E. Barnekow, and A.M. Phillips. 2007. Measuring flux of soil fumigants using the aerodynamic and dynamic flux chamber methods. *J. Environ. Qual.* 36:613–620.
- Wang, D., S.R. Yates, F.F. Ernst, J. Gan, and W.A. Jury. 1997. Reducing methyl bromide emission with a high barrier plastic film and reduced dosage. *Environ. Sci. Technol.* 31:3686–3691.
- Wauchope, R.D., T.M. Butler, A.G. Hornsby, P.W.M. Augustijn-Beckers, and J.P. Burt. 1992. The SCS/ARS/CES Pesticide properties database for environmental decision-making. *Rev. Environ. Contamin. Toxicol.* 123:1–155.
- Wilson, J.D., and W.K.N. Shum. 1992. A re-examination of the integrated horizontal flux method for estimating volatilisation from circular plots. *Agric. For. Meteorol.* 57:281–295.
- Wilson, J.D., G.W. Thurtell, and G.E. Kidd. 1981. Numerical simulation of particle trajectories in inhomogeneous turbulence, I: Systems with constant turbulent velocity scale. *Boundary-Layer Meteorol.* 21:295–313.
- Wilson, J.D., G.W. Thurtell, G.E. Kidd, and E. Beauchamp. 1982. Estimation of the rate of gaseous mass transfer from a surface source plot to the atmosphere. *Atmos. Environ.* 16:1861–1867.
- Yagi, K., J. Williams, N.Y. Wang, and R.J. Cicerone. 1995. Atmospheric methyl bromide (CH₃Br) from agricultural soil fumigations. *Science* 267:1979–1981.
- Yates, S.R. 2009. Analytical solution describing pesticide volatilization from soil affected by a change in surface condition. *J. Environ. Qual.* 38:259–267.
- Yates, S.R., F.F. Ernst, J. Gan, F. Gao, and M.V. Yates. 1996. Methyl bromide emissions from a covered field: II. Volatilization. *J. Environ. Qual.* 25:192–202.
- Yates, S.R., J. Gan, D. Wang, and F.F. Ernst. 1997. Methyl bromide emissions from agricultural fields: Bare-soil, deep injection. *Environ. Sci. Technol.* 31:1136–1143.
- Yates, S.R., J. Knuteson, F.F. Ernst, W. Zheng, and Q. Wang. 2008. Effect of sequential surface irrigations on field-scale emissions of 1,3-dichloropropene (1,3-D). *Environ. Sci. Technol.* 42:8753–8758.
- Zheng, Y.J., L. Wan, Z.B. Su, H. Saito, K. Huang, and X.S. Wang. 2009. Diurnal soil water dynamics in the shallow vadose zone. *Environ. Geol.* 58:11–23.